JOC*Article*

Synthesis of a NO-Releasing Prodrug of Rofecoxib

F. Conrad Engelhardt,* Yao-Jun Shi, Cameron J. Cowden, David A. Conlon, Brenda Pipik, George Zhou, James M. McNamara, and Ulf-H. Dolling

Department of Process Research, Merck & Company, Inc., P.O. Box 2000, Rahway, New Jersey 07065-0900

conrad_engelhardt@merck.com

Received August 12, 2005

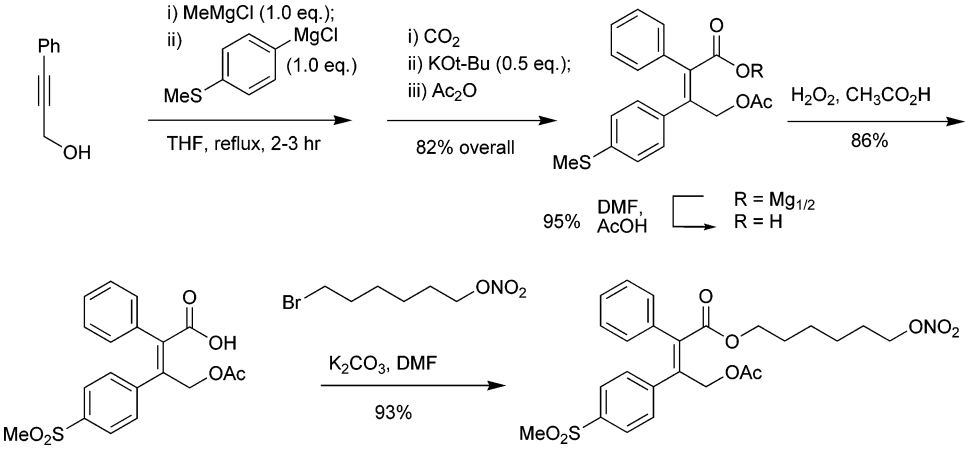

A newly developed synthesis of a NO-releasing prodrug of rofecoxib is described. The highly productive process consists of five chemical steps and produces prodrug **1** in an overall 64% yield from commercially available 3-phenyl-2-propyn-1-ol (**4**). The synthesis is highlighted by the carbometalation reaction of propargyl alcohol **4** to generate the tetrasubstituted olefin core, sulfone acid **2**. Additionally, two alternate end-game strategies to prepare NO−COXIB **1** from this intermediate were explored and developed: (1) a convergent synthesis where a bromonitrate side chain is introduced in one step and (2) a two-step sequence that first installs the requisite six-carbon ester side chain followed by chemoselective nitration.

Introduction

Nonselective nonsteroidal antiinflammatory drugs (NSAIDs) are widely used in the treatment of pain and arthritis, but these benefits are counterbalanced by gastrointestinal (GI) toxicity which is a common side effect of dual cyclooxygenase (COX-1 and COX-2) activity. This prompted the search for safer therapies, including the development of COX-2 selective inhibitors such as rofecoxib (VIOXX). Rofecoxib demonstrated high selectivity for the inhibition of the induced COX-2 isoform while sparing inhibition of the "housekeeping" COX-1, resulting in superior GI tolerability.

Although COX-2 inhibitors do not interfere with the anti-platelet activity of aspirin, they significantly increase the gastrointestinal injury caused by aspirin.[1] Currently, 26 million Americans take low-dose aspirin daily to reduce their risk of a cardiovascular event and, because of the potential of increased GI damage, are unable to benefit from the advancements offered by COX-2 selective drugs. Awareness of these protective effects and the emerging incompatibility of a low-dose aspirin regimen with COX-2 selective inhibitors led to the development of a new class of drugs, the COX inhibiting nitric oxide donators (CINODs). CINODs are a new class of antiinflammatory and analgesic drugs that may minimize gastrointestinal toxicity compared with standard nonsteroidal antiinflammatory drugs (NSAIDs) by virtue of this nitric oxide donation. This drug class is characterized by a COX inhibiting drug or prodrug linked to a nitric oxide moiety. In animal studies, CINODs lead to marked reductions in gastroduodenal and small bowel injury. Data have suggested that CINODs have the potential to be clinically beneficial with an improved gastrointestinal safety profile that will open up the possibility of codosing with patients who take low-dose aspirin.

(1) Fiorucci, S.; Santucci, L.; Wallace, J. L.; Sardina, M.; Romano, M.; Soldado, P.; Morelli, A. *Proc. Natl. Acad. Sci. U.S.A.* **2003**, *88*, 10937−10941.

10.1021/jo051712g CCC: $33.50
Published on Web 12/17/2005

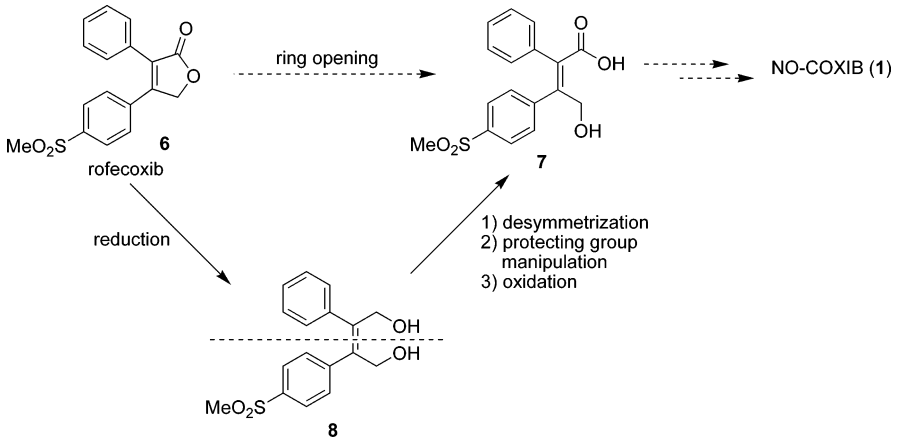

FIGURE 1. Rofecoxib starting material.

SCHEME 1. Prodrug for Rofecoxib (VIOXX) and Nitric Oxide

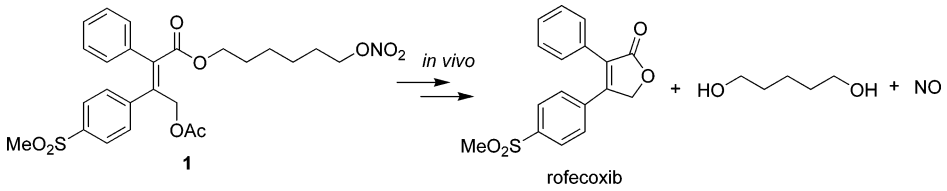

SCHEME 2. Retrosynthetic Analysis

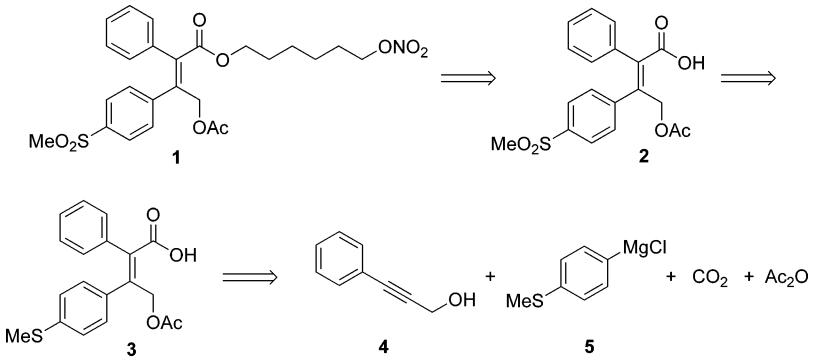

The novel CINOD (**1**) shown in Scheme 1 is a prodrug for both rofecoxib (VIOXX) and nitric oxide. Under physiological conditions, the acetate will be removed via esterase activity and subsequent ring closure will release the COX-2 selective inhibitor, rofecoxib. Additionally, the released side chain is expected to generate 1,6-hexanediol and nitric oxide (Scheme 1).

The novel COX-2 selective, nitric oxide compound **1** was in development for the treatment of pain, while hopefully being gastric sparing. As part of our program toward the synthesis of prodrug **1**, a convergent strategy was envisioned where a nitrate-containing C_6 side chain could be directly coupled to the (*Z*)-4-alkoxybut-2-enoic acid core **2** (Scheme 2). In turn, methyl sulfone **2** could be accessed by simple oxidation of the sulfide acid **3** precursor. The key step to the synthesis, however, is the one-pot construction of the tetrasubstituted alkene core of **1** using a Grignard carbometalation reaction between aryl Grignard **5** and propargyl alcohol **4**.

The regio- and stereocontrolled preparation of tetrasubstituted alkenes remains a difficult synthetic challenge. Recently, work by Fallis and co-workers highlighted the versatility and power of magnesium-mediated carbometalation reactions to access well-defined olefin systems. Inspired by this work, we examined the use of a magnesium-mediated carbometalation reaction to prepare (*Z*)-2,3-biaryl-4-acetoxybut-2-enoic acid[2] to gain access to NO-containing COX-2 inhibitors such as **1**. In this paper, we report the successful implementation of this approach and discuss alternate end-game strategies to completing the synthesis of NO-containing **1** from the sulfide acid **3**.

Results and Discussion

(*Z*)-2,3-Biaryl-4-hydroxybutenoic acid **7** represents a good entry point to the new class of NO−COXIB inhibitors (Figure 1).[3] Rofecoxib (**6**) appeared to be the ideal starting material, as it already contained the requisite biaryl-*Z*-olefin along with the appropriate carboxylic acid and allyl alcohol oxidation states (Figure 1). Unfortunately, any attempts to prepare ring-opened products directly using rofecoxib were unsuccessful. Although ring opening was difficult, reduction of rofecoxib was possible yielding the pseudosymmetric diol **8**. Unfortunately, this molecule still required a desymmetrization reaction, a protecting group manipulation, and oxidation to arrive at the desired (*Z*)-

(2) The synthesis of a series of (*Z*)-2,3-biaryl-4-acetoxybut-2-enoic acids was reported in International Patent Publication WO 96/13483 (1996).

(3) Internal communication with Merck Medicinal Chemistry.

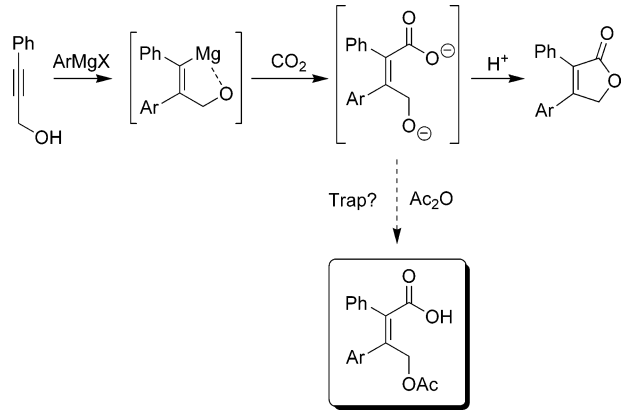

FIGURE 2. Proposal to trap the carboxylate/alkoxide intermediate.

2,3-biaryl-4-hydroxybutenoic acid **7**. Through these challenges, it became evident that rofecoxib was not the ideal starting material; instead, we focused our attention on other methodologies to prepare hydroxybut-2-enoic acid **7**.

As previously mentioned, Fallis has described a method for preparing 2,3-disubstituted butenolides,[4] including rofecoxib, via Grignard-mediated carbometalation chemistry with propargyl alcohols (Figure 2). Monosubstituted butenolides and saturated γ-lactones have also been prepared in a similar fashion using a hydromagnesiation reaction.[5] Presumably, preparation of these butenolides proceeds through a (*Z*)-4-alkoxybut-2-ene carboxylate intermediate prior to ring closure (Figure 2). Trapping and isolation of these tetrasubstituted alkene intermediates have not previously been described in the context of carbometalation chemistry. We report that these reactive intermediates can be intercepted using acetic anhydride to generate a (*Z*)-2,3-biaryl-4-acetoxybut-2-enoic acid **3**, the core of prodrug **1**. The four-component coupling strategy employed herein involves the addition of an aryl Grignard reagent **5** to 3-phenyl-2-propyne-1-ol **4** followed by a carbon dioxide quench and an acetate trap (Scheme 2). Naturally, challenges arose in the implementation of such a complex strategy. Each challenge will be addressed with particular emphasis on the installation of the carboxylic acid moiety and the subsequent preparation of the acetate-protected allylic alcohol intermediate.

We initially examined the use of 4-thiomethylphenylmagnesium chloride **5** and 3-phenyl-2-propyn-1-ol **4** to prepare vinyl Grignard intermediate **9** (Scheme 3). Further treatment of this magnesium chelate **9** with excess carbon dioxide followed by acetic anhydride generated (*Z*)-2,3-biaryl-4-acetoxybut-2-enoic acid **3**, albeit in low yield (6%), with a majority of the reaction mixture being comprised of the following side-product impurities (Scheme 3). Among the byproducts was thioanisole **10** which is generated from the initial deprotonation of 3-phenyl-2-propyn-1-ol with aryl Grignard **5**. Alkenes **12a,b** can be explained by incomplete reaction of vinyl Grignard **9** with carbon dioxide followed by a protic workup or acetate quench. Thioanisic acid **11** results from the reaction of excess aryl Grignard **5** with carbon dioxide. Finally, lactone **13** results from rapid ring closure of the carboxylate/alkoxide (Figure 2) after inefficient trapping with acetic anhydride. Despite low yields for the desired product **3**, we were encouraged by these initial results and systematically investigated the carbometalation reaction sequence in its three parts: (1) the carbometalation, (2) the carboxylic acid installation, and finally (3) the acetate trap.

1. Carbometalation. Several concerns emerged regarding the carbometalation step: (1) the preparation of Grignard reagent **5** from the less reactive aryl chloride, (2) the excess aryl Grignard reagent required, and (3) the use of a mixed-solvent system. Fallis and co-workers routinely report the use of chloro-based aryl and vinyl Grignard reagents in the carbometalation reaction. They note that the bromo-derived Grignard reagents consistently give *lower* yields than the chloro counterparts.[6] This was an issue as aryl bromides are preferable for the preparation of Grignard reagents because they are cheaper and more reactive than the corresponding aryl chlorides. It is also generally easier to prepare a Grignard reagent from the bromide precursor. We investigated whether there was a significant advantage in using a chloride-based Grignard reagent in this reaction. Our experiments[7] confirmed the observations by Fallis indicating that the Grignard reagents derived from aryl or vinyl chlorides are superior reagents in the carbometalation reaction. The chloride-derived Grignard reagent reacted more rapidly than the corresponding bromo Grignard to give the desired vinyl Grignard intermediate **9**, and the reaction was generally cleaner with fewer byproducts observed. One possible rationale for this difference is the potential presence of an unfavorable Schlenk equilibrium that may exist in the bromo Grignard case.[8]

Aware of the advantages of employing an aryl chloride Grignard, we turned to the preparation of 4-thiomethylphenylmagnesium chloride **5** from 4-chlorothioanisole **14** (Scheme 4). In the initial procedure, 4-chlorothioanisole **14** was added to a suspension of magnesium (~20 mesh, 1.25 equiv) and 1,2-dibromoethane (2.5 mol %) in refluxing THF (Scheme 4). These conditions always resulted in generation of 4-thiomethylphenylmagnesium chloride **5**, but the reaction was unpredictable; the problem was controlling the initiation of the reaction, a critical factor for large scale. Typically, 20−60% of the 4-chlorothioanisole **14** had to be charged to observe any reaction. Although there was never a propensity toward a runaway reaction, we sought to control the onset of the Grignard formation as a safety priority. It was discovered that the addition of 1−2 mol % of the product Grignard **5** to the system was the

(4) Fallis, A. G.; Wilson, P. D.; Forgione, P. *Tetrahedron Lett.* **2000**, *41*, 17−20.

(5) Takayori, I.; Okamoto, S.; Sato, F. *Tetrahedron Lett.* **1990**, *44*, 6399−6402.

(6) Fallis, A. G.; Wong, T.; Tjepkema, M. W.; Audrain, H.; Wilson, P. D. *Tetrahedron Lett.* **1996**, *37*, 755−758.

(7) A rate study in a mixed solvent system (cylcohexane/THF 1:3) confirmed that the 4-thiomethylphenylmagnesium chloride **5** reacted more quickly and cleanly than the bromo derivative both at room temperature (23 °C) and at reflux in THF (65 °C). The reaction employing the chloro-based Grignard reagent also went to completion within 4 h, whereas the bromo-based reagent stalled at 40−50% conversion and could not be driven further towards completion.

(8) For a discussion of Schlenk equilibrium of Grignard reagents, see: (a) Dessy, R. E.; Green, S. E. I.; Salinger, R. M. *Tetrahedron Lett.* **1964**, *21*, 1369−1374. (b) Smith, M. B.; Becker, W. E. *Tetrahedron* **1966**, *22*, 3027−3036. (c) Smith, M. B.; Becker, W. E. *Tetrahedron* **1967**, *23*, 4215−4227.

Schlenck Equilibrium

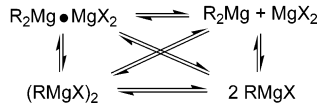

The preparation of a 2 M solution of 4-thiomethylphenylmagnesium bromide in THF resulted in a heterogeneous solution with significant precipitates observed. Alternatively, the 4-thiomethylphenylmagnesium chloride reagent, also prepared as a 2 M solution in THF, appeared homogeneous.

SCHEME 3. (*Z*)-2,3-Biaryl-4-acetoxybut-2-enoic Acid via Carbometalation and Acetate Trapping

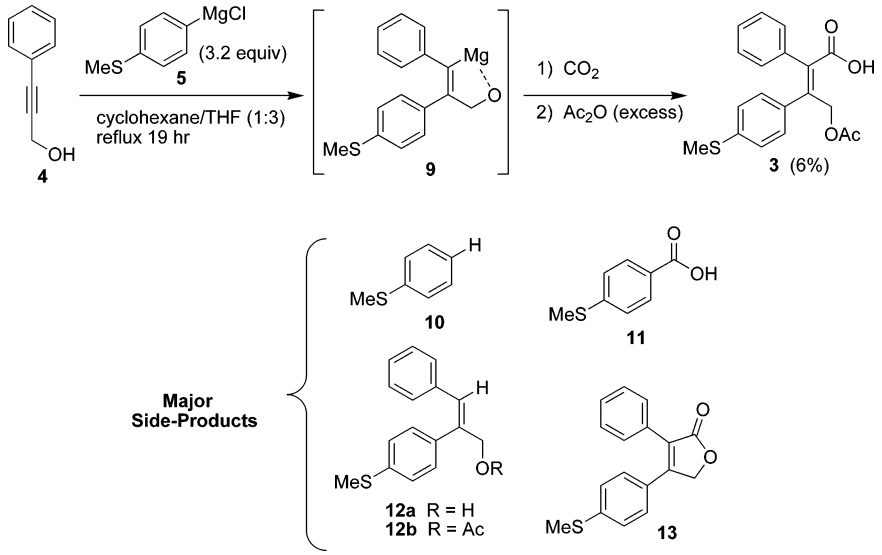

SCHEME 4. Preparation of 4-Thiomethylphenylmagnesium Chloride

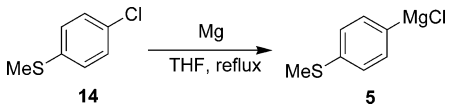

best, often providing controlled initiation using only a 5−10% initial charge of aryl chloride **14**.[9] Later, accumulated kinetic data alleviated any remaining safety concerns over the preparation of this aryl Grignard and confirmed that the reaction could be controlled.

The use of excess (3.2 equiv) expensive chloro Grignard reagent employed in the carbometalation step was a concern, especially as 1 equiv simply serves as a "sacrificial base" deprotonating propargyl alcohol **4**. A significant improvement was made by substituting a sacrificial alkyl[10] Grignard reagent, MeMgCl, for the deprotonation of the alkynol **4**.[11] The rate and reactivity profile for the subsequent Grignard carbometalation reaction after employing methylmagnesium chloride (1.00 equiv) as a sacrificial base matched what was seen previously with no new byproducts observed. This modification allowed us to reduce the charge of our more valuable 4-thiomethylphenylmagnesium chloride **5** from the previous 3.2 equiv routinely reported in the literature to only 1.1 equiv and resulted in a much cleaner reaction.[12]

After investigating the nature of the Grignard reagent, the effects of other variables in the carbometalation reaction were examined. Fallis routinely reports the use of a mixed-solvent system requiring a nonpolar solvent such as cyclohexane or toluene used in conjunction with THF (Scheme 3).[13] In accordance with the literature procedure, initial studies of the carbometalation reaction were run in a two-solvent system (cyclohexane/THF). However, it has been shown that in limited cases THF can work as the sole solvent.[14] Following this lead, we explored the use of a single solvent (THF) in these reactions and found that only 3−4 h is necessary to affect full conversion to vinyl Grignard intermediate **9** under these conditions.

To summarize, the new developments to the carbometalation step include: (1) demonstration of the superiority of the chloro-based Grignard reagent, (2) implementation of a sacrificial base, MeMgCl, for the initial deprotonation, (3) reduction in the charge of 4-thiomethylphenylmagnesium chloride (1.1 vs 3.2 equiv), and (4) simplification by employing THF as the sole solvent in the reaction. When all of these improvements were combined, the carbometalation step provided intermediate **9** (>95% conversion) in just 4 h at 65 °C in THF (Scheme 7).[15]

2. Carboxylic Acid Installation and Acetate Trap. With access to vinyl Grignard intermediate **9**, we looked to the next

(9) This method has the advantage of being indigenous to the process and introduces no new chemical entities to the system. Tilstam, U.; Weinmann, H. *Org. Process Res. Dev.* **2002**, *6*, 906−910.

(10) It has been shown that in the absence of copper iodide (CuI) alkyl Grignard reagents do not readily participate in the carbometalation reaction. See the following: (a) Tessier, P. E.; Penwell, A. J.; Souza, F. E. S.; Fallis, A. G. *Org. Lett.* **2003**, *5*, 2989−2992. (b) Douboudin, J. G.; Jousseaume, B.; Saux, A. *J. Organomet. Chem.* **1979**, *168*, 1−11.

(11) Initially, *i*-PrMgCl was used as the sacrificial base, but an excess charge of this reagent ultimately led to the generation of a mixed anhydride and the difficult to reject isobutyl ester impurity upon reaction with dianion **15** (see below). This problem was mitigated by substituting methylmagnesium chloride as the sacrificial Grignard reagent. In this case, excess MeMgCl generated acetate upon reaction with carbon dioxide and subsequent reaction with acetic anhydride would simply regenerate acetic anhydride, which would still allow formation of the desired (*Z*)-4-alkoxybut-2-enoic acid **3** (see below).

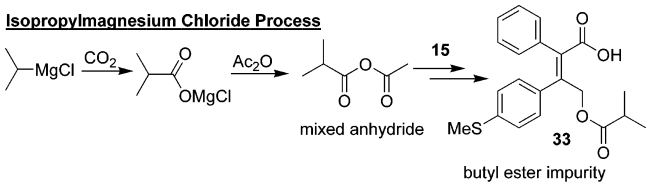

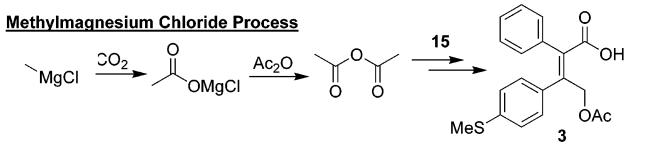

(12) The amount of thioanisole **10** and thioanisic acid **11** byproducts has been reduced significantly by employing an alkylmagnesium chloride reagent (MeMgCl) as a sacrificial base. The only byproduct now is methane gas.

(13) Previous investigations have suggested that solvent plays an important role in these carbometalation reactions. Nonpolar solvents such as cyclohexane were essential for the direct condensation of the magnesium chelate intermediate with aldehydes. Toluene/THF mixtures (1:1) have been shown to provide significant improvements in some reactions.

(14) Forgione, P.; Fallis, A. G. *Tetrahedron Lett.* **2000**, *41*, 11−15.

SCHEME 5. Unoptimized Acetate Trapping of an Alkoxide Intermediate

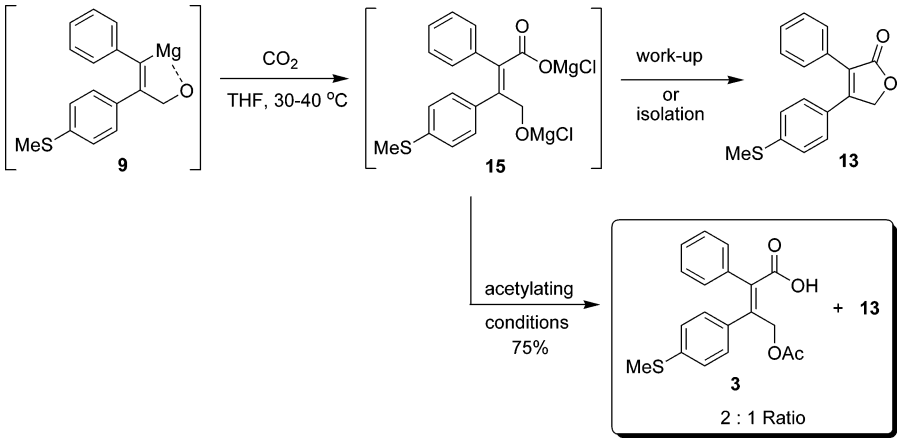

steps of the reaction sequence: (1) installation of the carboxylic acid moiety and (2) trapping of the alkoxide intermediate (Scheme 2). Using the optimized conditions described above, we generated vinyl Grignard intermediate **9** and then treated it with carbon dioxide[16] to afford the (*Z*)-4-hydroxybut-2-enoic acid[17] in high yield. The final step in the one-pot reaction sequence, the interception of the proposed reactive intermediate carboxylate/alkoxide dianion **15**[18] via trapping with an acetylating reagent, proved the most challenging to understand. A variety of acetylating agents including AcCl, Ac_2O, AcCN,[19] and AcBr were investigated, and the best results were achieved using Ac_2O. Adding excess acetic anhydride (2.0 equiv) to carboxylate/alkoxide **15** at 30 °C afforded the desired acid **3** in ~50% yield along with ~25% of butenolide **13** (Scheme 5). Initial efforts[20] to improve the yield of **3** while minimizing **13** were unsuccessful. Over the course of these early studies, the overall yield of the reaction (product **3** *plus* lactone **13**) was consistently high (70−90%), independent of any alterations in acylation conditions, and the ratio of product **3** to lactone **13** was typically 2:1.[21] Lactone **13** most likely results from inefficient trapping of dianion intermediate **15**; however, we were concerned that it may form competitively with **3** under the acetylation reaction conditions. Reaction monitoring using ReactIR indicated that under the reaction conditions *no* butenolide[22] **13** was formed prior to or during the acetic anhydride quench (Figure 2), and only upon protic workup was **13** observed (25% yield).[23]

In addition to monitoring lactone **13**, the ReactIR revealed that a significant amount of "free" carbon dioxide (2330−2350 cm^{-1}) remained dissolved in the THF (ca. 0.25 M at 25 °C) after all of vinyl Grignard intermediate **9** was consumed. Further observation of the carbon dioxide signal showed that over time the concentration of free CO_2 in solution slowly declined (Figure 2) but could not be accounted for in the headspace of the reaction, indicating that the gas was reacting in solution. We were also able to show that increasing the age after introduction of carbon dioxide had a detrimental effect on the overall yield of the reaction and reduced the ratio of product **3** to lactone **13** after trapping with acetic anhydride.[13] Taking all of this information into account, we proposed the following: excess free CO_2 in the reaction system may be slowly reacting with the alkoxide anion of **15** to form a carbonate species **16**, in essence protecting the allylic alkoxide from subsequent acetylation. Subsequent protic workup after Ac_2O introduction releases carbon dioxide, and the resulting (*Z*)-4-hydroxybut-2-enoic acid cyclizes rapidly to provide butenolide **13** (Chart 1).[24]

Variation of the temperature, concentration, and solvent led to only a slight change in the ratio of product to lactone, so attention was turned instead to the introduction of additives to the reaction system, primarily with the intent of removing the carbon dioxide from the system in an effort to prevent formation of carbonate **16**. It was the addition of alkoxide bases (0.5 equiv) such as NaOEt or KO^{t}Bu that gave encouraging results, as the percent of lactone **13** in the reaction product mixture was reduced from the typical 30−35% to 15 and 11%, respectively.

Again, in situ ReactIR experiments were conducted, this time, to understand the critical role potassium *tert*-butoxide plays in

(15) As assayed by quenching into methanol and quantifying trisubstituted alkene **12a**.

(16) The CO_2 quench is best performed by bubbling excess CO_2 through the reaction mixture while maintaining a slightly elevated temperature range (30−40 °C) to afford a reasonable reaction rate. Although lower temperatures facilitate carbon dioxide solubility in THF, incorporation of the carbon dioxide moiety was significantly reduced.

(17) (*Z*)-4-hydroxybut-2-enoic acid **7** cannot be isolated, and it cyclizes upon protic workup to give butenolide **13**. The presence of butenolide **13** serves as a viable assay for the presence of (*Z*)-4-hydroxybut-2-enoic acid in this step.

(18) ReactIR confirmed that butenolide **13** (C=O: 1758 cm^{-1}) is not present under the reaction conditions and is generated only upon protic workup. For reference, the carbonyl stretch for the opened carboxylate/alkoxide **15** is much broader (1650−1500 cm^{-1}).

(19) (a) Cain, B. R. *J. Org. Chem.* **1976**, *41*, 2029−2031. (b) Holy, A.; Soucek, M. *Tetrahedron Lett.* **1971**, *2*, 185−188.

(20) The reaction at the acetate quench stage was evaluated in different solvent systems (THF, MeCN, toluene, and DMF). The effect of temperature on the reaction was also evaluated (0 °C, 22 °C, and 100 °C). Finally, additives such as bases (^{n}BuLi, KHMDS, CaH_2, and Hunig's Base) and Lewis Acid salts ($CaCl_2$, LiCl, LiBr, KBr, KCl, $MgBr_2$, NaI, and $ZnCl_2$) were added to try to alter the ratio of desired acid **3** to lactone **13**. Encouragingly, variability in the ratio of **3**/**13** was observed under all of these various reaction conditions; unfortunately, the best ratio observed was 2:1, and thus, 30−35% of the product mixture was being lost as the lactone **13** byproduct.

(21) The ratio of desired acid **3**/butenolide **13** was 2:1. Efforts to increase this ratio were unsuccessful.

(22) Butenolide **13** slowly grew (1758 cm^{-1}) but amounted to only a 0.7% yield over the course of 14 h in the presence of carbon dioxide.

(23) The final amount of butenolide **13** observed at the end of the reaction increased in direct proportion to the length of the carbon dioxide age prior to the acetylation step. Longer carbon dioxide exposures (i.e., >3 h) had a detrimental effect on the ratio of acid **3** to lactone **13**.

(24) Gas evolution has been observed upon the addition of acetic anhydride on larger scales supporting the notion of the carbonate protecting group. Longer carbon dioxide exposures prior to the acetate trapping step resulted in an increase in the observed butenolide **13**, presumably due to a larger concentration of carbonate **16**. Also, free carbon dioxide is observed after acetic anhydride is added to the system.

CHART 1. IR Showing Carbonate Formation

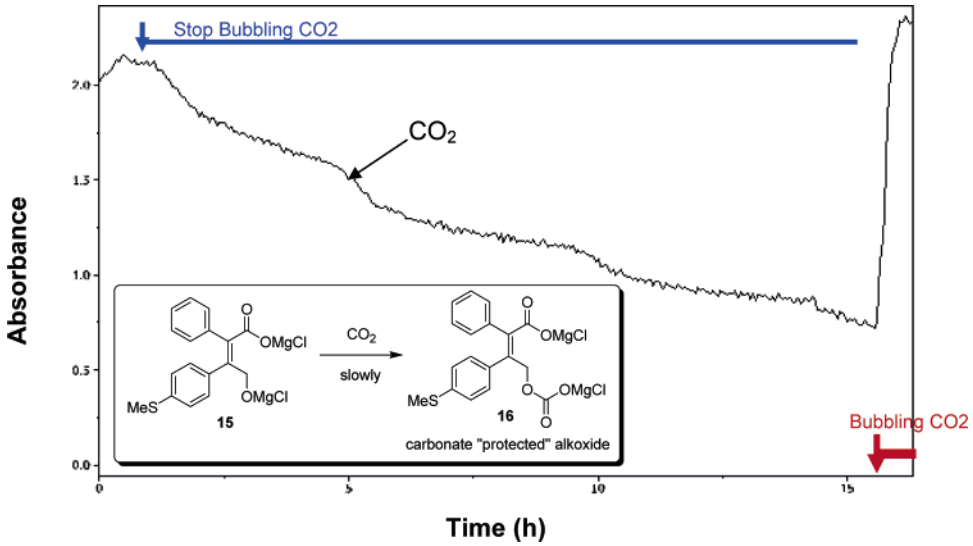

SCHEME 6. Increased Product to Lactone Ratio in the Absence of Carbon Dioxide

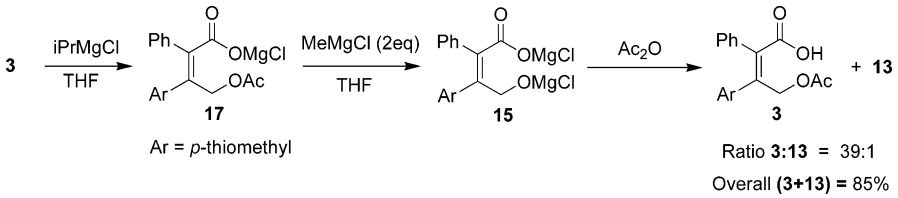

suppressing the formation of butenolide **13**.[25] It is believed that potassium *tert*-butoxide acts as a carbon dioxide scavenger sequestering CO_2 as a *tert*-butyl carbonate species.[26] An experiment was designed to access both the carboxylate **17** and the alkoxide **15** in a controlled manner from the sulfide acid **3** while monitoring the intermediate species with the ReactIR (Scheme 6). Adding isopropylmagnesium chloride (1 equiv) to the sulfide acid **3** cleanly afforded carboxylate **17**, and subsequent addition of 2 equiv of methylmagnesium chloride generated the dianion alkoxide **15** with an end of reaction observed after 45 min (the reaction could be monitored by observing the decay of the acetate signal at 1740 cm^{-1}). Finally, quenching with an excess of acetic anhydride cleanly afforded carboxylate **17** *with no IR evidence of lactone **13***. Protic workup and HPLC analysis confirmed a ratio of >39:1 (**3**/**13**) for this reaction in 85% yield. This experiment verified that acetate/acid **3** could be obtained in high yield by intercepting dianion intermediate **15** using an acetate trap.

TABLE 1. Carbon Dioxide Effect on Product to Lactone Ratio (3/13)

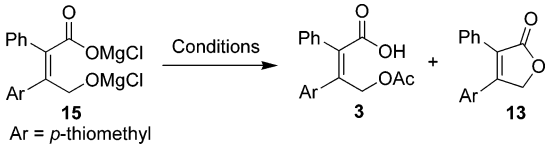

entry	conditions	ratio **3**/**13**	yield (%)
1	(a) CO_2 (30 min, room temperature) (b) Ac_2O (excess, room temperature)	2.5:1	63
2	(a) CO_2 (30 min, room temperature) (b) KO^{t}Bu (0.50 equiv) (c) Ac_2O (excess, room temperature)	14:1	86
3	(a) CO_2 (30 min, room temperature) (b) KO^{t}Bu (0.50 equiv) (c) CO_2 (30 min, room temperature) (d) Ac_2O (excess, room temperature)	3.5:1	65

The experiments in Table 1 were designed to generate the same intermediate, alkoxide **15**, and to probe the effect residual carbon dioxide has on the ratio of product **3**/lactone **13**. Entry 1 showed that exposing alkoxide **15** to carbon dioxide prior to the acetate quench significantly impacted the yield (**3** + **13**) of the reaction (63%) and reduced the ratio of product to lactone (2.5:1). Entry 2, on the other hand, went a step further and attempted to negate the detrimental effect of carbon dioxide exposure by "scrubbing" the reaction solution with potassium

(25) Spectral information garnered from the ReactIR experiment described in Scheme 6. Each compound has a unique infrared C=O stretching frequency that can be readily distinguished from other reactive intermediates. Note that the carbonyl of both the acid and the acetate protecting group can be used to identify each intermediate.

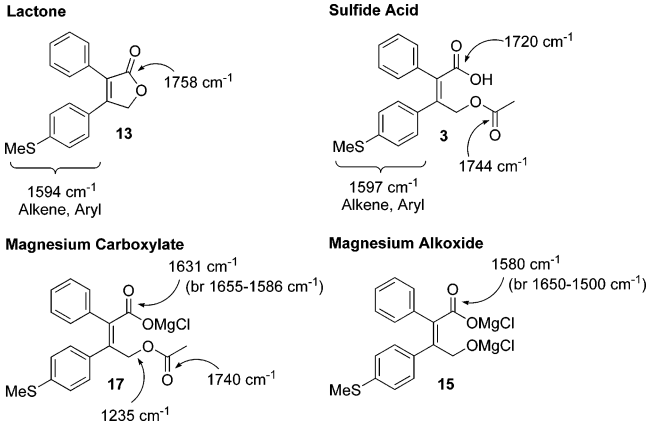

(26) All other attempts to remove the carbon dioxide from the reaction medium, including purging, sparging, and thermal techniques, have failed to give favorable results.

SCHEME 7. Optimized Carbometalation Step

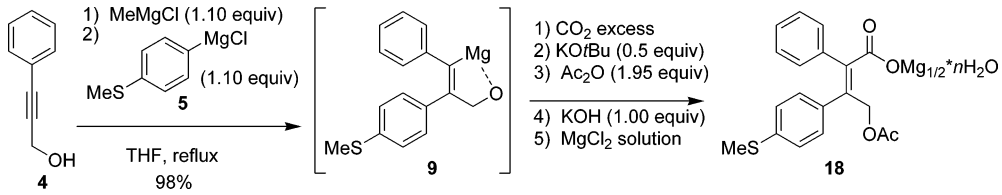

CHART 2. IR Response of CO_2 at 2350 cm^{-1}

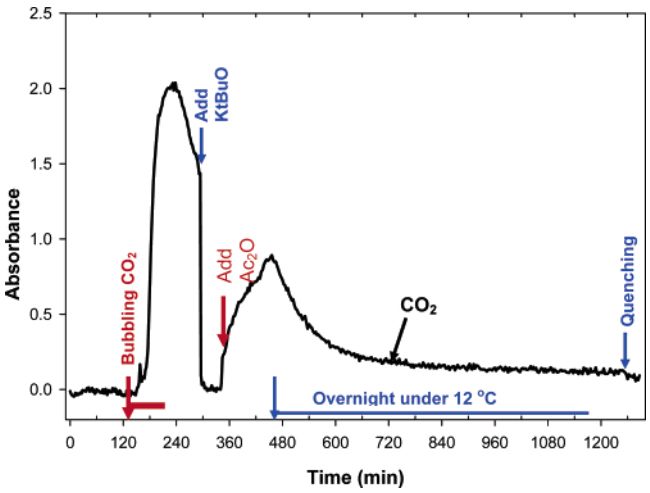

tert-butoxide. During the experiment, the carbon dioxide peak is observable at 2339 cm^{-1} and corresponds to free gas in the THF solution. The addition of potassium *tert*-butoxide resulted in an immediate and sharp decrease in the concentration of CO_2 (see Chart 2). At this point, acetic anhydride was added and the reaction was quenched. The overall yield of the reaction under these conditions rebounded to 86%, and the ratio of product **3** to lactone **13** increased (14:1). The observed ratio and shown decrease in free CO_2 in solution due to the addition of potassium *tert*-butoxide support the conjecture that this additive acts as a carbon dioxide scavenger. This effectively "deprotects" alkoxide **15** allowing for efficient acetate quenching to afford the desired trapped intermediate **17**. The last experiment in the table, entry 3, examines whether the detrimental effect of carbon dioxide returns when CO_2 is reintroduced after scrubbing the reaction with KO^{t}Bu. A significant amount of butenolide **13** was generated under these conditions again with a lower yield (65%). This implies that excess carbon dioxide is detrimental to the success of the reaction, and adding the appropriate amount[27] of potassium *tert*-butoxide is critical. Upon the introduction of the mildly acidic acetic anhydride, the *tert*-butoxide sequestered CO_2 is rendered unstable and is released into solution (see Chart 2), further confirming that there is a reservoir of carbon dioxide covalently bound as a carbonate species.

Having achieved high solution assay yields for acid **3**, we addressed the next issue of how to isolate the sulfide acid in the presence of numerous byproducts including thioanisic acid and butenolide **13** (3−6%) without resorting to chromatography. We were fortunate to discover that acid/acetate **3** could be isolated as a pure[28] crystalline solid by an in situ preparation of the corresponding magnesium salt **18** (Scheme 7). This was accomplished in practice by first buffering the crude reaction mixture with KOH[29] after the acetic anhydride quench and then washing with an aqueous magnesium chloride solution.[30] Upon separating the layers and adding an antisolvent (i.e., MTBE, EtOAc, and IPAc) to the THF layer, a solid crystallized. Pursuit of this isolation procedure led to the optimized protocol where water[31] was added and isopropyl acetate (2 volumes) was used as the antisolvent for crystallization. The highly productive carbometalation reaction fully optimized now allowed for the isolation of >99% pure magnesium salt as a hydrate in high yield from readily available starting materials. This one-pot sequence of reactions constructs the entire carbon backbone of our targeted NO−COXIB, leaving only a sulfide to sulfone oxidation and nitrate side chain incorporation (Scheme 2).

The entire optimized process for the carbometalation procedure includes the following: (1) a one-pot, single solvent (THF) process; (2) MeMgCl as a sacrificial base; (3) 4-thiomethylphenylmagnesium chloride (1.10 equiv); (4) Ac_2O as the acetylating agent; (5) KO^{t}Bu (0.5 equiv) as an additive to "scrub out" excess CO_2; (6) a pH adjust using KOH; and (7) formation and isolation as the hydrated magnesium salt **18**. The optimum conditions routinely provided **18** in 85% isolated yield and 99% purity (Scheme 7).

3. Salt Break and Oxidation. Although direct oxidation of magnesium salt **18** was possible, the oxidation step was plagued with low yields and erratic results due to the presence of magnesium[32] (2.5 wt %) and chloride.[33] A salt break step was introduced to convert magnesium salt **18** to the free acid **3** and to remove these inorganic impurities. The salt break was easily achieved by dissolving the magnesium salt **18** in DMF and adding to it a 2 M aqueous solution of acetic acid at 40 °C (Scheme 8). Free acid **3** prepared by this procedure contained <100 ppm of metals and chloride and was typically >99 LCAP.

(27) The amount of KO^{t}Bu added to the carbometalation reaction is optimized on the basis of the volume of THF in the reaction and the solubility of CO_2 in THF at ambient temperature (ca. 0.25 M). Calculations based on the volume of THF and the solubility of carbon dioxide provided the insight to the appropriate amount of KO^{t}Bu (0.5 equiv) that needs to be added.

(28) Typical purity was >98.5% by HPLC analysis at 210 nm.

(29) Mother liquor losses during the isolation of the magnesium salt had been variable and high (6−25%). Work revealed that the liquor losses were closely tied to the pH of the crystallization solution. Potassium hydroxide (aqueous, 30−45 wt %) was added to the crude reaction to buffer the pH of the solution in the range of 6.4−7.2, as acetic acid was generated after acetate trapping with Ac_2O. This resulted in reproducible mother liquor losses of 5−7% (~3 mg/mL). One equivalent of KOH proved optimum as larger charges resulted in a pH >7.4 which is basic enough to generate insoluble $Mg(OH)_2$ (upon introduction of the $MgCl_2$ solution), causing thick emulsions. KOH was selected as the base because of its low cost, and having potassium as the counterion introduces no new metal species into the reaction system that could interfere with our isolation of the desired magnesium salt product.

(30) The magnesium chloride (1.4 M) solution is prepared using $MgCl_2 \cdot 6H_2O$. (*Caution! Do not use $MgCl_2$ to prepare an aqueous solution of $MgCl_2$, as introduction of water is potentially explosive because of the extremely high exothermic heat of solvation for this salt.*) The $MgCl_2$ solution serves mainly as an aqueous wash for the THF layer, and the high molarity of the solution allows facile separation between the aqueous and THF (organic) layers.

(31) Water (3−5% volume) was critical to the success of the crystallization, as the isolated magnesium salt is a highly hydrated species requiring 8−10 water molecules per mole of salt.

SCHEME 8. Salt Break, Oxidation, and Initial End-Game

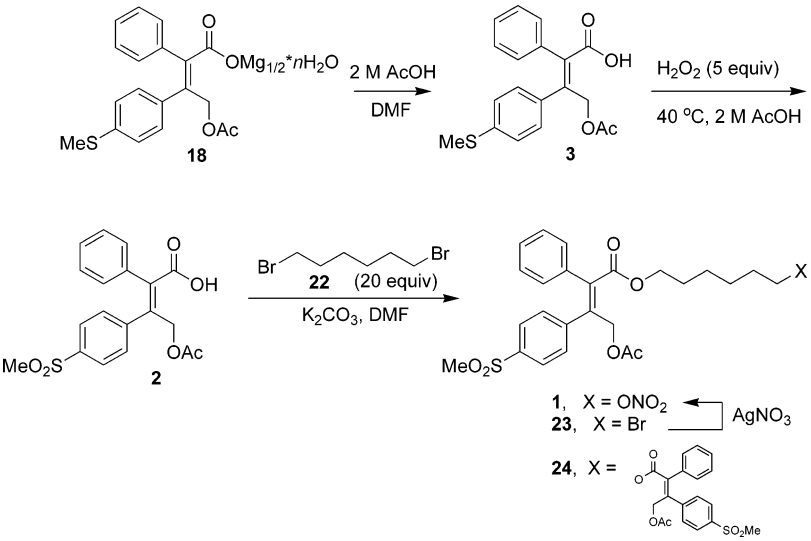

Many methods were examined for the oxidation of the sulfide acid **3** to the corresponding methyl sulfone **2**, including catalytic tungsten/H_2O_2, *m*CPBA, Oxone, MMPP, sodium perborate, and H_2O_2/acetic acid. The main problems with these methods included formation of rofecoxib **6**, isomerization of the double bond, oxidative cleavage of the double bond, and/or difficulty in isolating the sulfone acid **2** from the byproducts of the oxidation method. Hydrogen peroxide in acetic acid provided the most suitable oxidation conditions due to cost effectiveness, the ability to control the rate of reaction, and ease of product isolation. Hydrogen peroxide in acetic acid is regularly used as an oxidation system for the preparation of sulfones.[34] For large-scale reactions, we routinely avoid this system because of the possible generation of peracetic acid, a dangerous and potentially explosive compound. Using a ReactIR probe, we examined the reaction, which indicated that peracetic acid was not being produced under the reaction conditions (hydrogen peroxide in acetic acid at 40 °C). This process has now been demonstrated on a 50 kg scale to provide methyl sulfone **2** in >95% yield from sulfide acid **3** (Scheme 8).

To complete the synthesis, incorporation of the side chain remained. The initially reported procedure[35] coupled sulfone acid **2** with excess dibromohexane **22** to afford alkyl bromide **23**. Then, the final product was obtained by treating the primary bromide with silver nitrate[36] to afford NO−COXIB (**1**) (Scheme 8). A large excess of alkylating reagent and stoichiometric silver salt was used in an effort to minimize the formation of dimeric compound **24**. Unfortunately, despite the use of a 20-fold excess of 1,6-dibromohexane, impurity **24** was still observed (~4%) which necessitated extensive purification to remove this impurity from the final product. Two alternate end-game approaches were examined to avoid these complications and remove any exposure of the final compound to stoichiometric amounts of silver (vide infra).

End-Game Strategy. With the core of the molecule in hand, two alternate strategies for the final coupling of the side chain were explored. The first is a convergent approach (route A) where nitrate side chain **26** was prepared from 1,6-bromohexanol **25** and then coupled to sulfone acid **2** (Figure 3). This route, although initially attractive, suffered from the generation of the same difficult to remove impurities. The second strategy (route B) involves direct coupling of 1,6-bromohexanol **25** with acid **2** followed by nitration to yield prodrug **1**. Both coupling strategies will be discussed in detail below.

Convergent Strategy. The convergent synthesis of **1**, via route A, hinged upon the successful preparation of nitrate side chain **26** from 1,6-bromohexanol **25** and the subsequent coupling. To fully exploit the advantages of the convergent approach, a safe and economical synthesis of 6-bromohexyl nitrate **26** was needed. Additionally, as this compound is an oil, no purification of the product could be easily accomplished before coupling to give NO−COXIB (**1**), and hence, we needed to produce material as cleanly as possible. We initially used a H_2SO_4/HNO_3 nitration of 6-bromohexanol **26** under neat reaction conditions.[37] Although successful, obvious safety concerns emerged in response to this procedure. Alternatively, we turned to the use of an in situ prepared nitrating reagent, acetyl nitrate

(32) Under the harsh reaction conditions, 30% aqueous H_2O_2 (5 equiv) in AcOH at 40 °C, epoxidation of the *Z* olefin is possible in the presence of a metal catalyst such as magnesium. Hydrolysis of the formed oxirane followed by further oxidation can then lead to olefin cleavage products.

Oxidative Cleavage Products

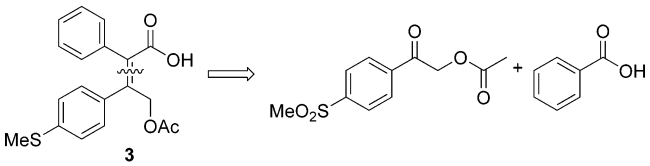

Other By-Products

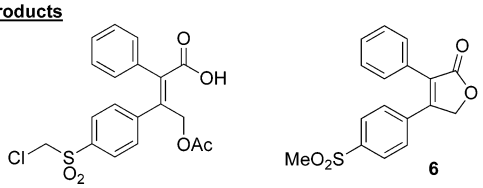

(33) Residual chloride (>200 ppm) in the sulfide acid salt led to the formation of chlorosulfone.

(34) Oxidation of aryl sulfides to aryl sulfones using hydrogen peroxide in acetic acid: Russell, G. A.; Pecoraro, J. M. *J. Org. Chem.* **1979**, *44*, 3990−3991.

(35) Internal communication with Merck Medicinal Chemistry.

(36) Reaction of an alkyl halide with silver nitrate to give a nitrate ester: Boschan, R.; Merrow, R. T.; van Dolah, R. W. *Chem. Rev.* **1955**, *55*, 485−510.

(37) Olah, G. A.; Malhotra, R.; Narang, S. C. *Nitration: Methods and Mechanisms*; VCH: New York, 1989 .

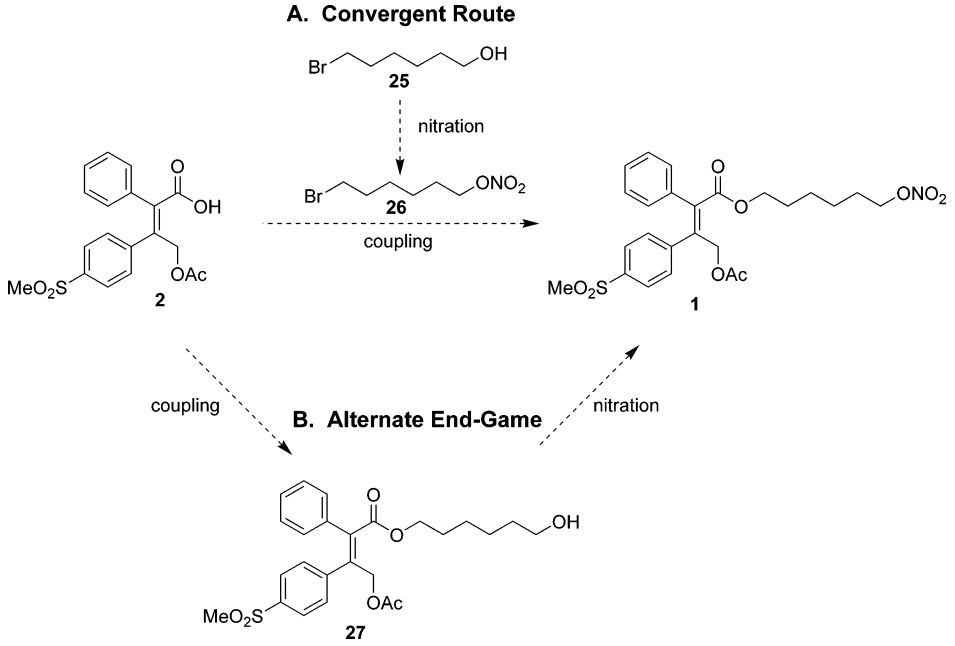

FIGURE 3. End-game strategy.

SCHEME 9. Preparation of 6-Bromohexyl Nitrate

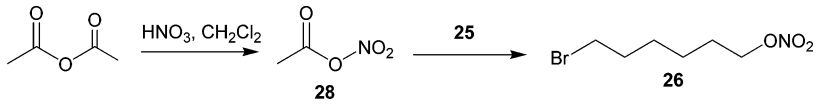

SCHEME 10. Convergent Coupling

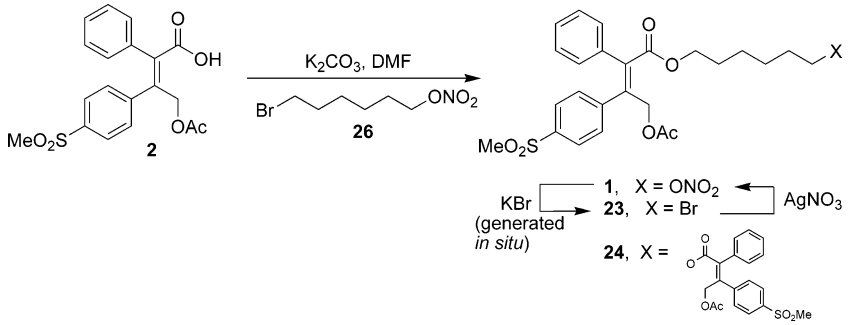

28 ($AcONO_2$),[38] formed from nitric acid (90%) and acetic anhydride[39] (Scheme 9). With an excess of acetyl nitrate **28** in the nitration step, the reaction cleanly afforded 6-bromohexyl nitrate **26** (Scheme 9), ready for use in the coupling step.

The coupling of sulfone acid **2** with prepared 6-bromohexyl nitrate **26** (2 equiv) was carried out using potassium carbonate (1.0 equiv) in DMF (10 volumes) at 20−22 °C. The reaction provided nitrate **1** after 2−3 h in 93% yield. Unfortunately, product **1** was also accompanied by two impurities, alkyl bromide **23** (∼2%) and dimer **24** (∼2%), both of which were not effectively rejected during a recrystallization of **1** (Scheme 10). Of major concern was the toxicity risk associated with having any bromide impurity **23** present in the final drug substance **1** as it is a potential active alkylating agent. Therefore, in practice, a silver nitrate treatment was implemented to convert bromide **23** into product **1** and silica chromatography was then used to remove the dimer **24**.

Although the coupling step initially appeared straightforward and high yielding (93%), the two impurities produced, bromide **23** and dimer **24**, cast a shadow on this process. Excellent chemoselectivity was observed in the coupling reaction, as the selectivity for bromide displacement by the carboxylate anion vs nitrate displacement was 124:1 (Scheme 11). Unfortunately, it is the combination of several unfavorable side reactions that leads to significant amounts of these two key impurities, bromide **23** and dimer **24** (vide infra).[40]

The origin of impurities **23** and **24** is relevant to any new synthesis, and their formation was shown to stem from multiple sources. Bromide impurity **23** emerges via two potential

(38) The generation of nitrating reagent $AcONO_2$ using acetic anhydride and nitric acid and its use in the nitration of an alcohol: Black; Babers *Organic Syntheses*, 1939; Vol. 19, pp 64−66.

(39) We have attempted to replace dichloromethane (DCM) with a more environmentally benign solvent, but we observed either overnitration or recovered starting material. So far, solvents tested include THF, DME, IPAc, chlorobenzene, MTBE, Ac_2O, CH_3CO_2H, and MeCN.

(40) We have not been able to reject either of these impurities by recrystallization without considerable yield losses of the desired final product.

SCHEME 11. Reaction Pathways in the Coupling of Sulfone Acid and 6-Bromohexyl Nitrate

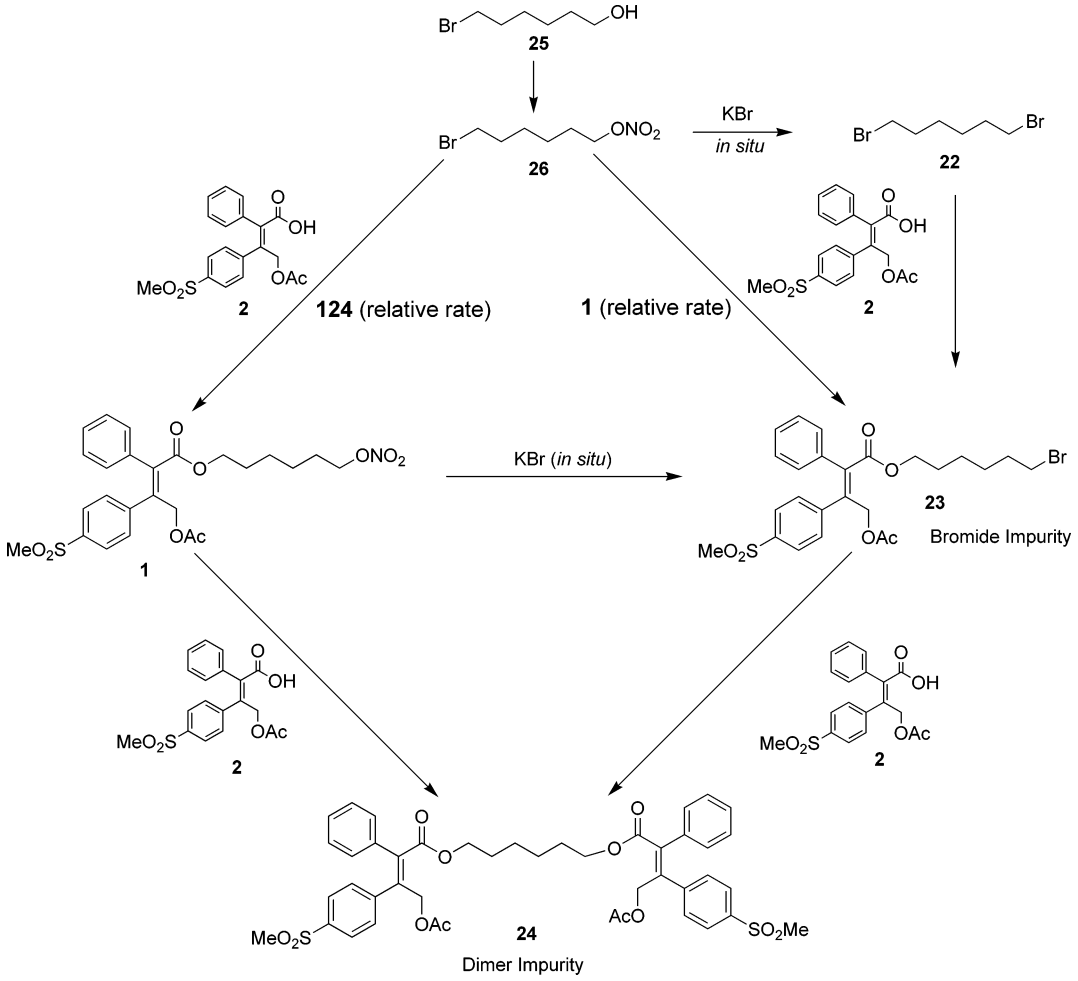

pathways; see Scheme 11. During the alkylation step, the nitrate group ($-ONO_2$) of **26** is susceptible to displacement by the carboxylate of sulfone acid **2** (Scheme 11), thus affording bromide **23**. Additionally, the nitrate group is also susceptible to displacement by a bromide ion (KBr) generated in situ from the coupling; thus, **1** can be converted directly to bromide **23**.

Similarly, the formation of the dimer impurity **24** can be rationalized (Scheme 11). The carboxylate of sulfone acid **2** can slowly displace the nitrate group of **1** during the alkylation reaction leading directly to dimer **24**. The primary bromide of any formed compound **23** can also be displaced by an unreacted carboxylate of sulfone acid **2**, leading to additional dimer **24**.

Alternative End-Game. The convergent route to NO−COXIB (**1**) incorporated the coupling of sulfone acid **2** with 6-bromohexyl nitrate **26** (Scheme 10); unfortunately, this reaction was complicated by side reactions (see Scheme 11) leading to two difficult to remove impurities, bromide **23** and dimer **24**. We sought a more controlled route to NO−COXIB (**1**) that would minimize formation of these impurities. We anticipated that coupling of sulfone acid **2** with 6-bromohexanol **25** would afford alcohol **27**, and without the presence of an electrophilic nitrate leaving group, bromide **23** and dimer **24** should not be generated. Two concerns emerged with this synthetic approach: (1) the potential instability of 6-bromohexanol under the basic coupling conditions, and (2) the chemoselectivity of the critical nitration of the primary alcohol in the presence of various sensitive functional groups including two aromatic rings. In practice, 1.10 equiv of 6-bromohexanol **25** coupled with sulfone acid **2** at 40 °C yielded alcohol **27** in 4−5 h (∼92% isolated yield) with no bromide impurity **23** and only small amounts of dimer **24** observed (<0.3% by HPLC analysis), resulting from the presence of 1,6-dibromohexane **22** as an impurity in commercial 6-bromohexanol **25**.

The nitration of alcohol **27** assumes greater importance in the newly improved synthesis as it becomes the final step. We initially found that competitive nitration of the phenyl group (compound **30** in Scheme 12) was problematic, but this was mitigated if the nitrating mixture (HNO_3/Ac_2O) was added to the substrate and if the temperature was controlled (−10 to −15 °C). In this case, the nitration leading to over-nitrated compound **30** was limited to <0.5% (by HPLC analysis) and this level was reduced to <0.1% upon crystallization to give **1**.[41]

As acetyl nitrate is documented[42] to be explosive at temperatures above 50 °C, we were concerned about its long-term use in our process. We thought that increasing the carbon content of the reagent would lead to a safer system and prevent the formation of the toxic tetranitromethane. Various anhydrides were examined (propionic, isobutyric, *n*-butyric, valeric, and hexanoic), and *n*-butyric anhydride was deemed optimal because

(41) Acetylation to give **29** was observed when the alcohol **27** was added rapidly to the nitrating mixture (HNO_3/Ac_2O), and as long as the addition time was extended to over 30 min, acetylation was completely suppressed.

(42) Butler, A. R.; Hendry, J. B. *J. Chem. Soc. B: Phys. Org.* **1971**, 102−105.

SCHEME 12. Coupling and Nitration: New and Improved Route

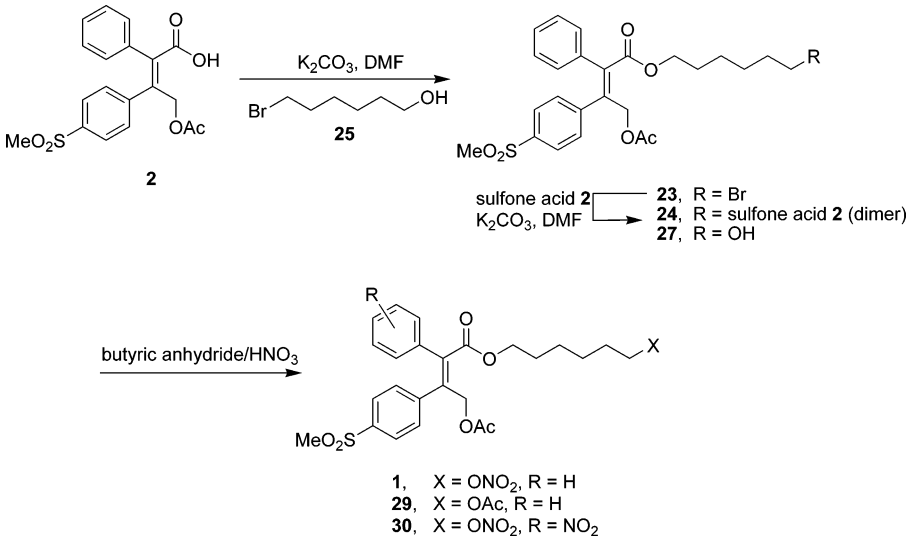

of its ease of workup, its reasonable rejection of any butyroyl ester formed, and the anticipated safety improvement (Scheme 12). With this modified procedure, the yield of isolated crude NO−COXIB (**1**) is generally 92−95% with excellent purity (>98%) as well.

Conclusions

Traditionally, tetrasubstituted alkenes with defined stereochemistries represent a challenging synthetic motif in organic chemistry. In this paper, we have demonstrated a highly efficient four-step one-pot carbometalation reaction that constructs a tetrasubstituted alkene with remarkable stereocontrol. The Grignard carbometalation reaction transforms a simple propargyl alcohol **4** into (*Z*)-2,3-biaryl-4-acetoxybut-2-enoic acid **3**, the core of prodrug **1**. Previously, this type of transformation has been used to prepare butenolides,[6] but we have shown that the intermediate (*Z*)-4-alkoxybut-2-ene carboxylate intermediate (Figure 2) can be intercepted with an appropriate acetate trap (Ac_2O). The optimization of this four-step process required an intricate understanding of the reaction intermediates which was obtained by using ReactIR. The sequestering of excess carbon dioxide by introducing an alkoxide base (potassium *tert*-butoxide) was instrumental in the success of the subsequent acetate trapping reaction to generate the opened product **3**. Finally, the synthesis of the NO−COXIB drug was completed via two different end-game strategies designed to control impurity and byproduct levels.

Experimental Section

Grignard Carbometalation. Magnesium Salt (18). A flask is charged with 300 mL of THF, and the vessel is flushed with nitrogen. This was followed by the addition of 66.1 g of 3-phenyl-2-propyn-1-ol (**4**). The batch was then cooled to approximately 5 °C, and 175 mL of methylmagnesium chloride (3 M, 1.05 equiv) was added slowly over 30 min, achieving a final batch temperature between 25 and 30 °C. Then, 268 mL of 4-thioanisolemagnesium chloride was added (2.05 M in THF, 1.10 equiv), and the batch was heated to reflux (65−70 °C). The batch was stirred at this temperature for 3 h and then was cooled to approximately 18 °C. Carbon dioxide (dry) was then charged subsurface, and the reaction was aged at 30 to 35 °C for 2 h.

The vessel pressure was then vented, and a series of purges were completed to remove residual carbon dioxide in the headspace. Then, 250 mL of potassium *tert*-butoxide (1 M in THF, 0.50 equiv) was charged to the homogeneous reaction mixture. The batch was stirred at 32 °C for 1 h. Finally, the batch temperature was adjusted to 23 °C and 94.5 mL of acetic anhydride (2 equiv) was added while maintaining a temperature of 30−45 °C. The batch was stirred for 1.5 h and then cooled to 10 °C. Then, the reaction was quenched with 93.5 mL of 30 wt % potassium hydroxide (28.1 g KOH, 1.0 equiv) and diluted with a deionized water flush (300 mL). The batch was aged at 40 °C for 7 h.

Next, 150 mL of an aqueous 2 M magnesium chloride solution was added and the batch was stirred for 15 min at 40 °C with strong agitation. Agitation was then ceased, and the two layers were allowed to settle and were separated. To the organic layer was added 100 mL of deionized water, and finally, 2.3 L of isopropyl acetate was added slowly over 2 h at 20 °C to complete the crystallization of the batch.

The batch was then cooled to 0 °C, and the slurry was filtered and washed with 500 mL of deionized water and 500 mL of cold (0 °C) isopropyl acetate. Filtration yielded 160.3 g of the desired crystalline hydrated magnesium salt product **18** (73.8% yield). Because of the various hydrate forms of the magnesium salt **18**, this compound was recrystallized as the free acid **3** in the subsequent step prior to full characterization (see below).

Salt Break. Carboxylic Acid (3). A solution of the magnesium salt **18** (2.63 kg corrected, 7.31 mol) in DMF (8 L) was slowly added to aqueous acetic acid (26 L, 2 M, 56 mol) at 35−40 °C. The precipitated free acid **3** was isolated by filtration, and the wet cake was washed with 20% aqueous DMF (6.6 L) and then twice with water (6.6 L). The product was dried at 40 °C under vacuum to yield 2.4 kg of the desired acid **3** as a tan crystalline solid (96% yield, mp = 149−150 °C). ^{1}H NMR (400 MHz, $CDCl_3$): δ (ppm) 10.87 (bs, 1H), 7.18−7.15 (m, 3H), 7.12−7.08 (m, 2H), 7.04−6.99 (m, 4H), 5.26 (s, 2H), 2.42 (s, 3H), 1.96 (s, 3H). ^{13}C NMR (100 MHz, $CDCl_3$): δ (ppm) 173.5, 171.2, 143.6, 138.8, 136.1, 134.4, 133.9, 130.0, 129.8, 128.3, 127.9, 125.7, 65.3, 20.8, 15.4. FTIR: (cm^{-1}) 3176, 3044, 2927, 1736, 1667, 1598, 1491, 1445, 1369, 1231, 1175, 1092, 1037, 815, 718, 706. HRMS calcd for $C_{19}H_{18}O_4S$ (M − H) *m*/*z* 341.0848, found 341.0846.

Protonated Intermediate (12a). This intermediate **12a** was recrystallized from hexanes (mp = 88−90 °C). ^{1}H NMR (400 MHz, $CDCl_3$): δ (ppm) 7.23−7.04 (m, 9H), 6.70 (s, 1H), 4.46 (d, J = 1.5, 2H), 2.50 (s, 3H), 1.68 (s, −OH, 1H). ^{13}C NMR (100 MHz, $CDCl_3$): δ (ppm) 141.0, 138.1, 136.6, 135.3, 129.5, 129.4, 128.2, 127.1, 127.0, 126.9, 68.7, 15.8. FTIR: (cm^{-1}) 3224, 3079, 3044, 3017, 2913, 2858, 1598, 1494, 1445, 1397, 1348, 1058, 815, 753, 698, 670. HRMS calcd for $C_{16}H_{16}OS$ (M + ^{7}Li) *m*/*z* 263.1082, found 263.1087.

Lactone (13) Byproduct. This impurity, **13**, was recrystallized from MTBE/THF (2:1) for characterization (mp = 144−146 °C). ^{1}H NMR (400 MHz, $CDCl_3$): δ (ppm) 7.45−7.37 (m, 5H), 7.24 (d, J = 8.7, 2H), 7.17 (d, J = 8.6, 2H), 5.17 (s, 2H), 2.49 (s, 3H). ^{13}C NMR (100 MHz, $CDCl_3$): δ (ppm) 173.7, 155.6, 143.0, 130.6, 129.5, 129.0, 128.9, 127.9, 127.0, 125.9, 125.6, 70.5, 15.1. FTIR: (cm^{-1}). HRMS calcd for $C_{17}H_{14}O_2S$ (M + H) *m*/*z* 283.0793, found 283.0789.

Sulfide Oxidation. Sulfone (2). A mixture of acid **3** (2.56 kg, 7.30 mol) in acetic acid (24 L) was heated to 40 °C, and hydrogen peroxide (3.26 L, 36.5 mol) was added over 15 min. After 6−8 h, the reaction was diluted with water (48 L). The mixture was seeded, and the temperature was held at 40 °C for 1 h and then allowed to cool slowly to room temperature over 2 h. The batch was then cooled further to −10 °C and held at this temperature for 1 h. The product was isolated by filtration, washed with 7 L of water, and dried under vacuum to afford sulfone acid **2** (2.46 kg, 89.8%) as a white crystalline solid (mp = 153−154 °C). ^{1}H NMR (400 MHz, $CDCl_3$): δ (ppm) 9.73 (bs, COOH, 1H), 7.75 (d, J = 8.6, 2H), 7.30 (d, J = 8.7, 2H), 7.20−7.14 (m, 3H), 7.08−7.05 (m, 2H), 5.28 (s, 2H), 3.00 (s, 3H), 1.95 (s, 3H). ^{13}C NMR (100 MHz, $CDCl_3$): δ (ppm) 172.2, 171.0, 143.5, 142.3, 139.7, 136.2, 134.9, 130.3, 129.8, 128.5 (2 peaks), 127.2, 64.9, 44.5, 20.8. FTIR: (cm^{-1}) 3190, 3079, 3024, 2927, 1736, 1598, 1494, 1445, 1307, 1231, 1155, 1099, 1085, 968, 781, 767, 663. HRMS calcd for $C_{19}H_{18}O_6S$ (M − H) *m*/*z* 373.0746, found 373.0747.

End-Game Strategy 1: Convergent Approach. A. Bromonitrate Preparation (26). Nitric acid (90% w/w) (1.45 kg, 20.7 mol) was added over 1 h to a solution of acetic anhydride (2.53 kg, 24.8 mol) in dichloromethane (20 L) maintained at −10 °C. This mixture was then stirred at 0 °C for 1 h before a solution of 6-bromohexanol **25** (2.50 kg, 13.8 mol) in dichloromethane (20 L) was added over 1.5 h, maintaining the temperature below 0 °C. The reaction was stirred for 30 min, quenched into K_2HPO_4 solution (10 L of 1 M), and stirred for 14 h before the layers were separated. The organic layers were washed with urea solution (5 L of 10% w/w solution), water (20 L), and brine (10 L of saturated aqueous). The organic solution was then concentrated to afford the crude 6-bromohexyl nitrate **26** (3.19 kg, 100 wt %, quant) as a colorless oil.

B. Coupling of Nitrate to Give NO−COXIB (1). To a 100 L flask was charged 20 L of DMF, solid sulfone acid **2** (2.72 kg, 6.97 mol), liquid bromonitrate **26** (3.99 kg, 17.2 mol), and 4.4 L of DMF to give a clear solution at room temperature. To this resulting solution was added powder K_2CO_3 (0.98 kg, 7.09 mol) in one portion at 20 °C, followed by 2.0 L of DMF for rinsing, and the mixture was then stirred at 20−22 °C for 2−3 h.

Next, ethyl acetate (30 L) was introduced and then cold water (30 L) was added slowly to maintain the temperature at <30 °C. The mixture was stirred for 0.5 h and settled to give two clear layers. The aqueous layer was separated and back-extracted with EtOAc (25 L). A combined organic layer was washed with water (2 × 20 L) and then saturated brine solution (26 L). The organic layer was concentrated in vacuo to ∼20 L, followed by addition of ∼20 L of *n*-heptane at 18−22 °C, and stirred for 1−2 h to provide a white slurry of the product. The remaining *n*-heptane (5 L) was introduced over 1 h to afford a thick slurry. The slurry was cooled to 0−5 °C to reduce the supernatant concentration to <1.5 mg/mL. It was then filtered, and the cake was washed with cold premixed EtOAc/*n*-heptane (1:3, 12 L) and air-dried at 23 °C under nitrogen for 12 h. The isolated white crystalline solid (3.56 kg) was obtained in 93.6% yield.

End-Game Strategy 2: Linear Approach. A. Preparation of Alcohol (27). To a 50 L glass vessel equipped with an overhead stirrer, a thermocouple, and a nitrogen inlet was charged 9 L of DMF, liquid bromohexanol **25**, solid sulfone acid **2**, and 2 L of DMF for rinsing to give a clear solution at room temperature. To this resulting solution was added powder K_2CO_3 in one portion at 20−22 °C, followed by 2 L of DMF for rinsing. Then, the solution was stirred at 20−22 °C for 10 min and then heated to 40−45 °C for 3−5 h.

The reaction mixture was cooled to ∼20 °C, and IPAc (26 L) was introduced. Then, ice-cold water (19 L) was added slowly to maintain the temperature at <30 °C. The mixture was stirred for 0.5 h and settled to give two clear layers. The aqueous layer was separated and back-extracted with IPAc (19 L). The combined organic layer was washed with water (2 × 19 L). The organic layer was concentrated in vacuo to ∼13 L and flushed with 13 L of IPAc. The resulting solution's concentration was adjusted to 170−180 mg/mL (∼15 L, KF <200 μg/mL). To this solution was added 5.5 L of *n*-heptane at 20−24 °C, followed by addition of ∼25 g of the seed (∼1 wt % based on 95% yield), and the solution was stirred for 1−2 h to provide a good seed bed (supernatant ∼50 mg/mL) at 18−20 °C. The remaining *n*-heptane (16.5 L) was introduced over 1−2 h and then aged for an additional 8 h. The slurry was cooled to −5 to 0 °C to reduce the supernatant concentration to <1.5 mg/mL. It was then filtered, and the cake was washed with cold premixed IPAc/*n*-heptane (1:4, 8 L) and air-dried at 22 °C under nitrogen for 12 h. The isolated crystalline solid (2.58 kg, 95 wt %) was obtained in 90% yield (mp = 59−62 °C). ^{1}H NMR (400 MHz, $CDCl_3$): δ (ppm) 7.70 (d, J = 8.5, 2H), 7.29 (d, J = 8.5, 2H), 7.12−7.07 (m, 3H), 7.01−6.97 (m, 2H), 5.11 (s, 2H), 4.20 (t, J = 6.6, 2H), 3.55 (t, J = 6.5, 2H), 2.96 (s, 3H), 1.98 (bs, −OH, 1H), 1.92 (s, 3H), 1.64 (quintet, J = 6.8, 2H), 1.49 (quintet, J = 6.8, 2H), 1.30 (m, 4H). ^{13}C NMR (100 MHz, $CDCl_3$): δ (ppm) 170.5, 168.0, 143.7, 139.4, 139.0, 137.6, 135.1, 130.3, 129.4, 128.3, 128.1, 127.1, 65.7, 64.7, 62.6, 44.4, 32.5, 28.4, 25.7, 25.3, 20.7. FTIR: (cm^{-1}) 3543, 3058, 2934, 2864, 1743, 1722, 1598, 1445, 1376, 1314, 1238, 1141, 1092, 1078, 961, 850, 753, 732, 704. HRMS calcd for $C_{25}H_{30}O_7S$ (M − H) *m*/*z* 473.1634, found 473.1636.

Nitration: Synthesis of NO−COXIB (1). Nitric acid (HNO_3) (344.6 mL, 7.33 mol) was added over 20 min to a cooled solution of *n*-butyric anhydride (1.375 kg, 8.69 mol) in dichloromethane (10 L) with the internal temperature remaining below 5 °C. After stirring for 2 h at 0 °C, the solution, to be cooled to −15 °C, and a solution of alcohol **27** (2.20 kg, 4.64 mol) in dichloromethane (7.3 L) was added over 30 min, maintaining the temperature below −10 °C. The reaction was stirred at −15 °C for 30 min. The reaction was quenched by addition of K_3PO_4 solution (8 L of 2 M aqueous solution). Then, toluene (10 L) was added and the layers were separated. The organic layer was washed with aqueous urea (20 L of 0.5%) and then solvent was switched to toluene (24 L final volume). The resulting toluene solution was filtered through a plug of silica gel (3.72 kg) with toluene/EtOAc elution (50 L of 90:10 mixture). Concentration of the eluent to 20 L volume was followed by addition of heptane (2 L) at 35 °C to obtain a seed bed. Further addition of heptane (17 L) was made, and filtration gave crude **1**. This material was recrystallized from toluene/heptane to give pure **1** as a white crystalline solid (2.05 kg, 90% yield, mp = 79−80 °C). ^{1}H NMR (400 MHz, $CDCl_3$): δ (ppm) 7.72 (d, J = 8.4, 2H), 7.30 (d, J = 8.4, 2H), 7.15−7.09 (m, 3H), 7.04−6.98 (m, 2H), 5.14 (s, 2H), 4.38 (t, J = 6.6, 2H), 4.22 (t, J = 6.5, 2H), 2.98 (s, 3H), 1.94 (s, 3H), 1.66 (quintet, J = 6.7, 4H), 1.40−1.27 (m, 4H). ^{13}C NMR (100 MHz, $CDCl_3$): δ (ppm) 170.5, 168.0, 143.7, 139.6, 139.4, 137.5, 135.2, 130.4, 129.5, 128.3, 128.2, 127.2, 73.2, 65.5, 64.7, 44.4, 28.3, 26.7, 25.5, 25.3, 20.8. FTIR (cm^{-1}): 2941, 2865, 1743, 1715, 1625, 1383, 1314, 1279, 1224, 1203, 1155, 1106, 1037, 961, 871, 705. HRMS calcd for $C_{25}H_{29}NO_9S$ (M − H) *m*/*z* 518.1485, found 518.1486.

Acknowledgment. Thanks to Roy Helmy and Peng Wang, our analytical team. Thanks to Liam Dunne and James Corry for the observation that potassium hydroxide buffers the pH to allow high yields from carbometalation reactions.

Supporting Information Available: Spectroscopic characterization (^{1}H, ^{13}C, and FT-IR) for compounds **1**−**3**, **12a**, **13** (^{1}H and ^{13}C only), and **27**. This material is available free of charge via the Internet at http://pubs.acs.org.

JO051712G